J. Phys.: Condens. Matter **22** (2010) 454109 (7pp) doi:10.1088/0953-8984/22/45/454109

Entropic transport of finite size particles

W Riefler[1], G Schmid[1], P S Burada[2] and P Hänggi[1]

[1] Institut für Physik, Universität Augsburg, Universitätsstraße 1, D-86135 Augsburg, Germany
[2] Max-Planck Institute für Physik komplexer Systeme, Nöthnitzer Straße 38, 01187 Dresden, Germany

E-mail: Gerhard.Schmid@physik.uni-augsburg.de

Received 1 April 2010, in final form 1 June 2010
Published 29 October 2010
Online at stacks.iop.org/JPhysCM/22/454109

Abstract
Transport of spherical Brownian particles of finite size possessing radii $R \leqslant R_{\max}$ through narrow channels with varying cross-section width is considered. Applying the so-called Fick–Jacobs approximation, i.e. assuming fast equilibration in the direction orthogonal to the channel axis, the 2D problem can be described in terms of a 1D effective dynamics in which bottlenecks cause entropic barriers. Geometrical confinements result in entropic barriers which the particles have to overcome in order to proceed in the transport direction. The analytic findings for the nonlinear mobility for the transport are compared with precise numerical simulation results. The dependence of the nonlinear mobility on the particle size exhibits a striking resonance-like behavior as a function of the relative particle size $\rho = R/R_{\max}$; this latter feature renders possible new effective particle separation scenarios.

(Some figures in this article are in colour only in the electronic version)

1. Introduction

The diffusive behavior of Brownian particles depends mainly on their size, the interaction between them, and the environment where they are situated in. If, in addition to these characteristics, particles are confined within narrow, tortuous structures such as nanopores, zeolites, biological cells and microfluidic devices, the restriction of the space available for the particles will cause entropic barriers that will have strong impact on the diffusive behavior (cf [1] and references therein). Effective control schemes for transport in these systems require a detailed understanding of the diffusive mechanisms involving small objects and, in this regard, an operative measure to gauge the role of fluctuations. The study of these transport phenomena is, in many respects, equivalent to an investigation of geometrical constrained Brownian dynamics. As the role of inertia for the motion of the particles through these structures can typically be neglected, the Brownian dynamics can safely be analyzed by solving the Smoluchowski equation in the domain defined by the available free space upon imposing reflecting boundary conditions at the domain walls.

However, solving the boundary problem in the case of nontrivial, corrugated domains presents a difficult task. A way to circumvent this difficulty consists in coarsening the description by reducing the dimensionality of the system considering only the main transport direction, but taking into account the physically available space by means of an entropic potential [1–3]. The resulting kinetic equation for the probability distribution, the so-called Fick–Jacobs equation, is similar in form to the Smoluchowski equation, but contains now entropic contributions leading to genuine dynamics which distinctly differs from those observed for purely energetic potentials.

The driven transport of particles across bottlenecks [1–4], such as ion transport through artificial nanopores or artificial ion pumps [5–8] or in biological channels [9–12], are striking examples where the diffusive transport is regulated by entropic barriers. In addition, geometrical confinements and entropic barriers play also a prominent role in the context of the Stochastic Resonance phenomenon [13–17].

Our objective with this work is to investigate the mobility of noninteracting spherical Brownian particles in channels with varying cross-section width. In particular, we are interested in the influence of the particle size on the transport within a periodic entropic potential exhibiting barriers which arise from the geometrical restrictions.

The paper is organized as follows: in section 2 we introduce the model and define the theoretical and numerical problem. Further on, in section 3 we present the basic principles of the Fick–Jacobs approximation allowing for reducing the two-dimensional problem to an one-dimensional one. The results are presented in section 4. Finally, we give the main conclusions in section 5.

2. Modeling

Transport through pores or channels (like the one depicted in figure 1) may be caused by different particle concentrations maintained at the ends of the channel, or by the application of external forces acting on the particles. Here, we exclusively consider the case of force driven transport of spherical particles of radius R. The external force $\vec{F} = F\vec{e}_x$ is pointing parallel to the direction of the channel axis. As small deviation from this assumption does not affect our results, certainly not within the limits of validity of the Fick–Jacob approximation. Moreover, we shall assume low concentrations of spherical particles such that particle–particle interactions and all hydrodynamic interaction effects can consistently be neglected.

2.1. Dynamics inside the channel

In general the dynamics of a suspended Brownian particle is overdamped [18] and well described by the Langevin equation:

$$\eta_R \frac{\mathrm{d}\vec{r}}{\mathrm{d}t} = \vec{F} + \sqrt{\eta_R k_\mathrm{B} T}\vec{\xi}(t), \tag{1}$$

where $\vec{r}$ denotes the center position of the spherical particle in the two-dimensional channel, k_B the Boltzmann constant, T the temperature and $\vec{\xi}(t)$ is the standard 2D Gaussian noise with $\langle\vec{\xi}(t)\rangle = 0$ and $\langle\xi_i(t)\xi_j(t')\rangle = 2\delta_{ij}\delta(t-t')$ for $i, j = x, y$. The friction coefficient η_R is given by Stokes' law:

$$\eta_R = 6\pi\nu R \tag{2}$$

and depends on the shear viscosity ν of the fluid and the particle radius R. In addition to equation (1) the full problem is set up by imposing reflecting boundary conditions at the channel walls. The boundary of the 2D periodic channel which is mirror symmetric about its x-axis is given by the periodic function $y = \pm\omega(x)$ with $\omega(x + L) = \omega(x)$ where L is the periodicity of the channel. ω_min and ω_max refer to the half of the maximum and minimum channel width, respectively.

To further simplify the treatment of this problem, we introduce dimensionless variables. We measure all lengths in units of the periodicity of the channel, i.e. $x = x'L$. As a unit of time τ we choose twice the time it takes the largest transportable particle to diffusively cover the distance L which is given by $\tau = L^2\eta_\mathrm{max}/(k_\mathrm{B}T)$, hence $t = \tau t'$. The largest transportable particle is the particle with radius $R_\mathrm{max} = \omega_\mathrm{min}$. Accordingly, the friction coefficient of a particle of radius R is then given by $\eta = \rho\eta_{max}$ with the ratio of spherical particle radii being $\rho = R/R_\mathrm{max}$ and $\eta_\mathrm{max} = 6\pi\nu R_\mathrm{max}$.

Summarizing, the Langevin equation (1) reads in dimensionless variables:

$$\frac{\mathrm{d}\vec{r}'}{\mathrm{d}t'} = \frac{f}{\rho}\vec{e}_x + \sqrt{\frac{1}{\rho}}\vec{\xi}(t'), \tag{3}$$

where the dimensionless force parameter [2, 3]

$$f = \frac{LF}{k_\mathrm{B}T}. \tag{4}$$

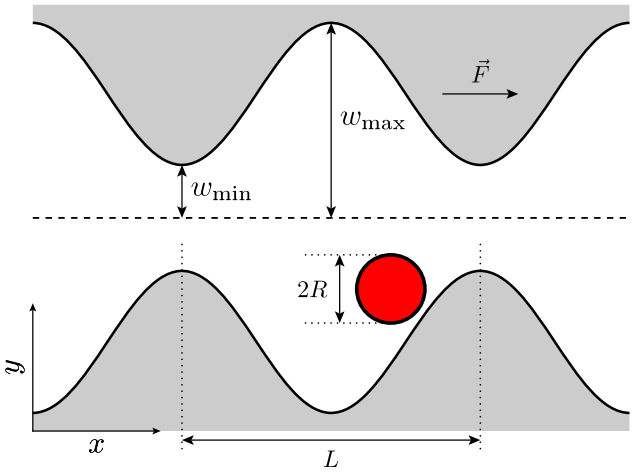

Figure 1. Sketch of the 2D periodic channel with periodicity L, the minimum half channel width ω_min and the maximum half channel width ω_max. The spherical Brownian particle of radius R is subjected to the force $\vec{F}$.

For the sake of better readability, we shall skip all the primes in the following and proceed, if not mentioned explicitly otherwise, with dimensionless variables.

The corresponding Fokker–Planck equation for the time evolution of the probability distribution $P(\vec{r}, t)$ takes the form [19]

$$\frac{\partial P(\vec{r}, t)}{\partial t} = -\vec{\nabla}\vec{J}(\vec{r}, t), \tag{5}$$

where $\vec{J}(\vec{r}, t)$ is the probability current:

$$\vec{J}(\vec{r}, t) = \frac{1}{\rho}\left(f\vec{e}_x - \vec{\nabla}\right)P(\vec{r}, t). \tag{6}$$

2.2. Boundary conditions

As the particles are confined by the channel structure, the probability current has to vanish at the boundaries. Due to the finite size of the particles their center position can approach the boundary only up to its radius. Consequently, the position vector $\vec{r}$ of a particle with radius R never approaches the channel walls and is restricted to only a portion of the inner channel area, cf figure 1. The *effective boundary function* $\omega^\mathrm{eff}(x)$, which serves as boundary for the center of mass, exhibits the distance R from the original, *true* boundary function $\omega(x)$. Consequently, the 'no-flow' boundary conditions for the center of mass dynamics read:

$$\vec{J}(\vec{r}, t)\cdot\vec{n} = 0\,, \quad \text{for} \quad \vec{r} \in \text{effective boundaries}, \tag{7}$$

where $\vec{n}$ denotes the normal vector field at the effective channel walls. For the considered 2D channel structure, the boundary condition becomes

$$\frac{\mathrm{d}\omega^\mathrm{eff}(x)}{\mathrm{d}x}\left\{fP(x, y, t) - \frac{\partial P(x, y, t)}{\partial x}\right\} + \frac{\partial P(x, y, t)}{\partial y} = 0, \tag{8}$$

at $y = \pm\omega^\mathrm{eff}(x)$.

Note, that the effective boundary function exhibits a complex dependence on the particle's radius R and could not

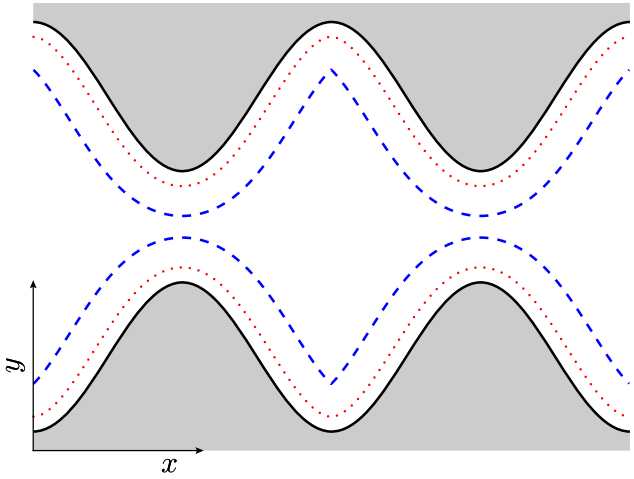

Figure 2. Sketch of the original tube geometry given by the boundary function $\omega(x)$ and the effective boundary function $\omega^{\text{eff}}(x)$ for the center of the spherical particle. Hereby, the effective boundary function depends on the radius of the particle which is given in dimensionless units by ρ: $\rho = 0.27$ (red dotted line), $\rho = 0.81$ (blue dashed line).

be given explicitly. If the curvature of the channel wall function $\omega(x)$ is larger than that of the particle, the effective boundary function exhibits a kink, cf figure 2.

For an arbitrary form of $\omega(x)$, the boundary value problem defined by equations (5), (6) and (8) is very difficult to solve. Despite the inherent complexity of this problem an approximate solution can be found by introducing an effective one-dimensional description where geometric constraints and bottlenecks are considered as *entropic barriers* [2, 4, 20–25].

3. Fick–Jacobs approximation

The 1D equation is obtained from the full 2D Smoluchowski equation upon the elimination of the transversal y coordinate assuming fast equilibration in the transversal channel direction.

3.1. The Fick–Jacobs equation

The marginal probability density along the axis of the channel is defined by

$$\mathcal{P}(x,t) = \int_{-\omega^{\text{eff}}(x)}^{\omega^{\text{eff}}(x)} P(x,y,t)\,\mathrm{d}y. \tag{9}$$

Assuming fast equilibration in y-direction the 2D probability distribution becomes

$$P(x,y,t) = \mathcal{P}(x,t)\,Q(y|x), \tag{10}$$

with the local equilibrium distribution $Q(y|x)$ of y, conditional on a given x. If there is no force component in transversal channel direction (as it is in our case), the conditional distribution $Q(y|x)$ is uniform and reads due to the normalization condition:

$$Q(y|x) = 1/(2\,\omega^{\text{eff}}(x)). \tag{11}$$

Then on integrating the full 2D Smoluchowski equation (5) and making use of equations (9), (10) and (11), the Fick–Jacobs equation for the spherical particle is obtained:

$$\frac{\partial\,\mathcal{P}(x,t)}{\partial x} = \frac{1}{\rho}\frac{\partial}{\partial x}D(x)\left\{\frac{\mathrm{d}A(x)}{\mathrm{d}x} + \frac{\partial}{\partial x}\right\}\mathcal{P}(x,t), \tag{12}$$

with the dimensionless free energy $A(x) = -f\,x - \ln 2\omega^{\text{eff}}(x)$. For a periodic channel this free energy assumes the form of a tilted periodic potential with the bottlenecks forming entropic potential barriers. Note, that for a straight channel, i.e. constant effective boundary function, the entropic contribution vanishes and the particle is solely driven by the external force.

Introducing the x-dependent diffusion coefficient $D(x)$ in equation (12) considerably improves the accuracy of the kinetic equation, extending its validity to more winding structures [21–25]. The expression for $D(x)$ (in dimensionless units)

$$D(x) \doteq \frac{1}{\left[1 + (\mathrm{d}\omega(x)/\mathrm{d}x)^2\right]^{1/3}}, \tag{13}$$

has been shown to appropriately account for curvature effects of the confining walls [22].

3.2. Nonlinear mobility

Besides the effective diffusion coefficient, the average particle current, or equivalently the nonlinear mobility serves as key quantity of particle transport through periodic channels. For any non-negative force the average particle current in periodic structures can be obtained from [26–28]

$$\langle\dot{x}\rangle = \langle t(x_0 \to x_0 + 1)\rangle^{-1}, \tag{14}$$

where $\langle t(a \to b)\rangle$ denotes the mean first passage time of particles starting at $x = a$ to arrive at $x = b$. Within the Fick–Jacobs equation (12), the mean first passage time can be determined:

$$\langle t(a \to b)\rangle = \rho \int_a^b \mathrm{d}x\,\exp(-f\,x)/\omega^{\text{eff}}(x) \times \int_{-\infty}^{x} \mathrm{d}y\,\exp(f\,y)\omega^{\text{eff}}(y). \tag{15}$$

The nonlinear mobility $\mu(f)$ is defined by $\mu(f) = \langle\dot{x}\rangle/f$ and can be obtained as

$$\mu(f) = \frac{1}{\rho}\cdot\frac{1-\exp(-f)}{f\int_0^1 \mathrm{d}z\,I(z,f)}, \tag{16}$$

where

$$I(z,f) = 1/D(z)\exp(-f\,z)/\omega^{\text{eff}}(z)\int_{z-1}^{z}\mathrm{d}y\,\exp(f\,y)\omega^{\text{eff}}(y). \tag{17}$$

In case of a straight channel with $\omega_{\min} = \omega_{\max}$, an exact analytical solution of the full 2D Smoluchowski equation (5) is known and the nonlinear mobility equals the free mobility (i.e. without geometrical constrictions)

$$\mu = \mu_{\text{free}} = 1/\rho = R_{\max}/R \quad \text{(for straight channels)}. \tag{18}$$

Consequently, the influence of the confinement can be expressed by the ratio of nonlinear mobility for the transport through the channel and the one for the unrestricted case:

$$\frac{\mu(f)}{\mu_{\text{free}}} = \frac{1-\exp(-f)}{f\int_0^1 \mathrm{d}z\, I(z,f)}. \tag{19}$$

4. Precise numerics for a two-dimensional channel geometry

The nonlinear mobility, predicted analytically within the Fick–Jacobs approximation, has been compared with Brownian dynamic simulations performed by a numerical integration of the full 2D Langevin equation (3), using the stochastic Euler algorithm. As random number generator we used the Box–Muller and MT19937 algorithm from the *GSL* library. The sinusoidal shape of the considered two-dimensional channel is described by

$$\omega(x) := a\sin(2\pi x) + b, \tag{20}$$

with the two dimensionless channel parameters a and b. In physical units, these two parameters are given by aL and bL, respectively. Note that $\omega(x)$ may also be regarded as the first terms of the Fourier series of a more complex boundary function. Due to the symmetry with respect to the x-axis, the boundary function could be given in terms of the maximum half-width $\omega_{\max} = b + a$ and the aspect ratio of minimum and maximum channel width $\epsilon = \omega_{\min}/\omega_{\max}$ (with $\omega_{\min} = b - a$), i.e.

$$\omega(x) = \frac{\omega_{\max} - \omega_{\min}}{2}\left[\sin(2\pi x) + \frac{\omega_{\max} + \omega_{\min}}{2}\right], \tag{21}$$

$$\omega(x) = \frac{\omega_{\max}}{2}(1-\epsilon)\left[\sin(2\pi x) + \frac{1+\epsilon}{1-\epsilon}\right]. \tag{22}$$

To ensure, that the spherical particles of radius ρ stay within this channel geometry, the integration was carried out performing 'no-flow' boundary conditions at the channel walls. By averaging over 10^5 simulations we obtain the steady-state average particle current

$$\langle \dot{x} \rangle = \lim_{t\to\infty} \frac{\langle x(t)\rangle}{t}, \tag{23}$$

and the nonlinear mobility $\mu = \langle \dot{x}\rangle / f$.

4.1. Nonlinear mobility: force and temperature dependence

Figure 3 depicts the nonlinear mobility as a function of the scaling parameter f for two different particle radii and a fixed channel geometry: $\omega(x) = 0.7/(2\pi)\sin(2\pi x) + 1.02/(2\pi)$. Strikingly, the transport through such channel structures is distinctly different from the one occurring in one-dimensional periodic *energetic* potentials [2–4, 29]. This phenomenon is due to the different temperature dependence of the barrier shapes. Decreasing the temperature in an energetic periodic potential decreases the transition rates from one cell to the neighboring one by decreasing the Arrhenius factor [30] and, therefore, reduces the nonlinear mobility. For the periodic channel system, a decrease of temperature results in an increase

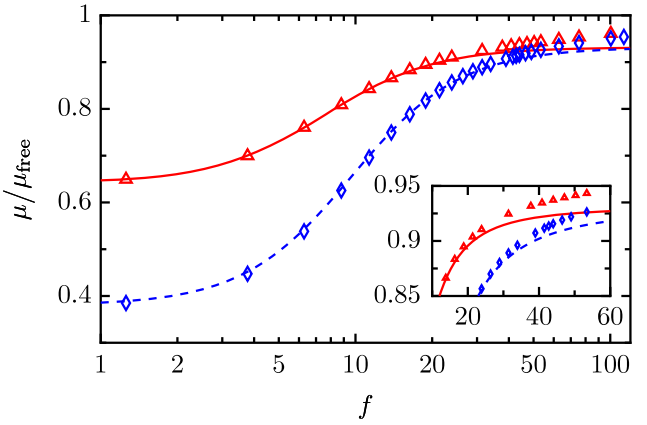

Figure 3. (Color online) Graph for the scaled nonlinear mobility as a function of the force parameter f. In the Langevin simulation the different symbols correspond to different particle radius of $\rho = 0.2$ (red triangles) and $\rho = 0.8$ (blue diamonds). The relative error of the simulation results is smaller than 0.01. The Fick–Jacobs results, equation (19), correspond to the solid lines. The boundary function reads: $\omega(x) = (0.7/2\pi)\sin(2\pi x) + 1.02/2\pi$.

of the dimensionless force parameter f, cf equation (4) and consequently, in a monotonic increase of the nonlinear mobility.

Due to the geometrical restrictions, the nonlinear mobility is always smaller than the mobility for the free case, cf figure 3. With increasing scaling parameter, the nonlinear mobility tends to that of the free case, i.e. $\mu \to \mu_{\text{free}}$ for $f \to \infty$.

A comparison of the analytics obtained by means of the Fick–Jacobs approximation with the precise numerics enables one to determine validity criteria for the Fick–Jacobs approximation, for further details see [3, 4]. According to them the applicability of the Fick–Jacobs approximation for the transport of point particles depends on the smoothness of the geometry and the scaling parameter f. For finite size particles, the diameter of the particles should become an additional parameter in the validity criteria. In particular, the particle's radius determines the maximum width of the effective channel structure. A larger particle leads to a smaller maximum effective width. Since for a fast equilibration in the orthogonal tube direction the timescale for the orthogonal diffusion process must be smaller than the timescale for the drift [3], a smaller maximum channel width favors the validity of the Fick–Jacobs approximation. Thus, with increasing particle size the range of the applicability of FJ increases, cf figure 3.

However, it turned out, that the transport phenomena presented below, occur for channel structures for which the validity criteria is not fulfilled. Therefore, we stick in the following, to the numerical results only.

4.2. Particle size

Surely, the transport of particles through small channel systems depends on the size of the particles. In particular, the effect of the size on the nonlinear mobility is two-fold. Firstly, the friction coefficient depends on the particle size, resulting in a ρ-dependence of the nonlinear mobility even for the case

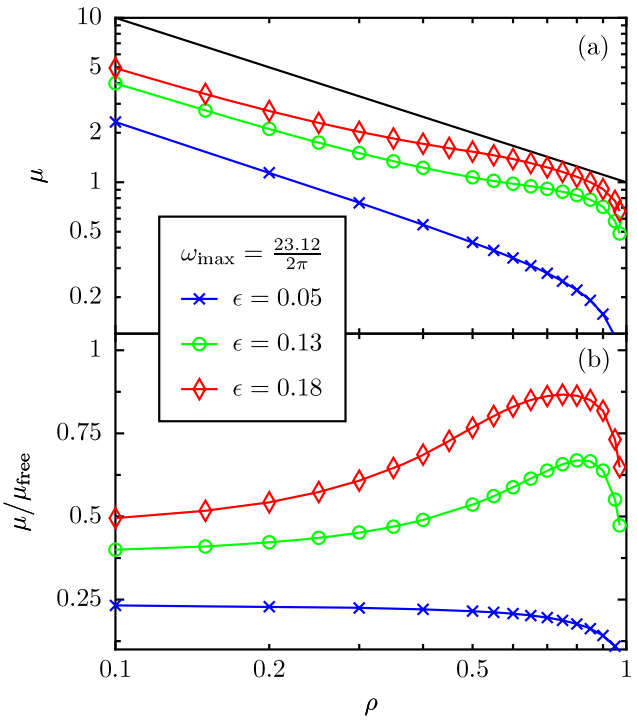

Figure 4. The numerically obtained nonlinear mobility μ (a) and the scaled nonlinear mobility μ/μ_{free} (b) as a function of the radii ratio $\rho = R/R_{\max}$ for different channel geometries (*constant-width-scaling*: $\omega_{\max} = \text{const}$), cf equation (22).

of unconstrained motion (free case), cf equation (18). With increasing radii ratio ρ, the mobility declines. Secondly, there is the influence of the geometrical confinement. The extent of the bottleneck ($2\omega_{\text{wmin}}$) gives a limit to the size of particles able to travel through the channel. In our scaling the largest sphere possible to overcome the geometry's bottleneck has a radii ratio of $\rho = 1$. Considering particles of different sizes, the effective bottleneck ($2\omega_{\min}^{\text{eff}}$) will be smaller for spheres of higher diameter. It is intuitive that a small bottleneck hinders the transport.

Figure 4(a) depicts the nonlinear mobility as a function of the radii ratio ρ for different geometries. For a straight channel one observes the nonlinear mobility of the free case μ_{free} which depends reciprocally on the radii ratio ρ. In presence of geometrical restrictions, i.e. for varying cross-section width, the nonlinear mobility is smaller than μ_{free}, cf figure 4(a). Moreover, upon decreasing the bottleneck half-width (i.e. decreasing the aspect ratio ϵ) of the structure, the nonlinear mobility decreases [31].

Deviations from the $1/\rho$-dependence show another effect of the geometrical confinement, cf figure 4(a). In order to focus on the geometrical effect, we consider the scaled nonlinear mobility, i.e. the nonlinear mobility relative to the nonlinear mobility in free case: μ/μ_{free}, cf figure 4(b). This is equivalent to the consideration of the nonlinear mobility of a point particle moving in the effective channel geometry defined by the effective boundary function $\omega^{\text{eff}}(x)$, which still depends on the parameter ρ. With increasing ρ, the maximum half-width of the effective geometry shrinks. As a consequence, the sojourn time, the particle spends on average in a bulge of the channel structure decreases with increasing ρ and the mobility of the point particle in the effective geometry grows. This behavior causes the maximum in the scaled nonlinear mobility and the shoulder in the dependence of the nonlinear mobility on the radius, cf figure 4.

4.3. Role of the channel structure

The confinement by the considered channel geometry can be altered by systematically changing the parameters $\omega_{\max}$ and $\omega_{\min}$ or $\omega_{\max}$ and ϵ in the boundary function, equation (21) or equation (22) respectively. While for figure 4 we examined a constant maximum half-width $\omega_{\max} = \text{const}$ and varied the aspect ratio ϵ which is equivalent to vary the half-width $\omega_{\min}$ at the bottleneck, cf the *constant-width-scaling* in [31], it is instructive to also consider both, the *constant-bottleneck-scaling* $\omega_{\min} = \text{const}$ as well as the *constant-ratio-scaling* $\epsilon = \omega_{\min}/\omega_{\max} = \text{const}$.

As we keep the bottleneck width constant and decrease the maximum half-width, the sojourn times the particles spends in the bulges decreases causing the mobility to increase and approach the maximum value for a straight channel ($\omega_{\min} = \omega_{\max}$ and $\epsilon = 1$), cf figure 5(a). In contrast, within the *constant-ratio-scaling*, where the bottleneck half-width scales with the maximum half-width, the nonlinear mobility μ depends for small radii only slightly on $\omega_{\max}$, cf figure 5(b). However, with increasing particle size, i.e. radii ratio ρ, the nonlinear mobility μ shows a striking dependence on the maximum half-width.

As pointed out already, with increasing particle radius the effective maximum half-width decreases. The effective maximum half-width will exhibit a linear dependence on the radius if the particle curvature is larger than that of the channel's boundary function (in physical units),

$$\omega_{\max}^{\text{eff}} = \omega_{\max} - R, \qquad \text{for } 1/R > \frac{-\mathrm{d}^2\omega(x_{\max})/\mathrm{d}x^2}{\left[1 + (\mathrm{d}\omega(x_{\max})/\mathrm{d}x)^2\right]^{3/2}}, \tag{24}$$

where $x_{\max}$ denotes the x-values for which the boundary function assumes a maximum. For larger particle radii the effective boundary function shows a kink and the effective maximum half-width $\omega_{\max}^{\text{eff}}$ decreases faster than linearly with the radii ratio ρ. As the sojourn times the particle spend in the channel's bulges depends mainly on the effective maximum width, a nonlinear dependence of the nonlinear mobility is observed for larger particle radii causing a peak in the scaled nonlinear mobility, cf figures 5(c) and (d).

5. Conclusions and outlook

We studied the transport of finite Brownian particles through channels with periodically varying width. For point size particles it was shown previously [3, 4], that the transport through such channels could be approximately described by means of the so-called Fick–Jacobs equation which is based on the assumption of a fast equilibration in orthogonal transport direction. Validity criteria for the capability of this approximation include a dependence on the channel shape and predict an upper limit for the force value. In case of spherical,

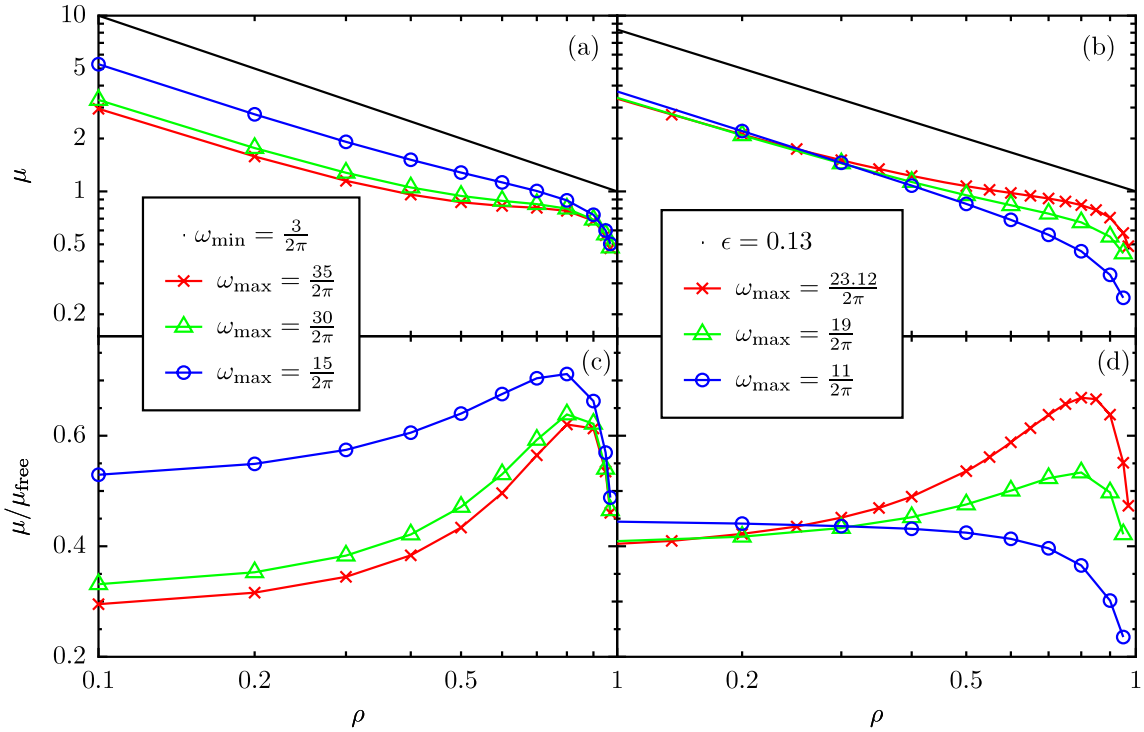

Figure 5. The nonlinear mobility (a), (b) and scaled nonlinear mobility (c), (d) are depicted for different scalings of the geometry: constant-bottleneck-scaling, i.e. $\omega_{\rm min} = \text{const}$, in (a) and (c); constant-ratio-scaling, i.e. $\epsilon = \omega_{\rm min}/\omega_{\rm max} = \text{const}$, in (b) and (d). The force parameter f equals 1.6π.

finite size particles the maximum force value up to which the Fick–Jacobs equation could be applied depends also on the size of the particle. By comparison of the approximative result for the nonlinear mobility and the numerical ones we have shown, that the equilibration assumptions holds for a wider force range in case of larger particles than it is the case for smaller ones.

In addition, we pointed out, that the transport of finite, spherical Brownian particles in channel geometries with highly corrugated channel walls exhibits some striking features which may allow for the development of newly separation devices which extends the functionality of the sieves. In particular we found, that the nonlinear mobility of Brownian particles in such channel structures deviates from the one-over-size dependence predicted by the Stokes law for Brownian particles moving in an environment without geometrical constrictions. Instead, there is an optimal particle size for which the nonlinear mobility as compared to the free mobility exhibits a maximum value.

Our present study also implicitly used a small concentration of spherical particles such that both, effects of particle–particle interactions and forces between particle–particle and particle–walls due to hydrodynamic interactions can safely be ignored. These complications would require totally new and extensive studies that are beyond this present study. Moreover, as emphasized in the abstract already, we assumed throughout perfect spherical symmetry. Deviations from such spherical symmetry would also impact the viscous friction law behavior [32] and, as well, may give rise to additional, new entropic effects. All such complications are beyond the work presented here; all these latter complications, however, open up avenues for interesting future investigations.

Acknowledgments

This work has been supported by the Volkswagen foundation (project I/83 902), the Max Planck society and by the German Excellence Initiative via the Nanosystems Initiative Munich (NIM).

References

[1] Burada P S, Hänggi P, Marchesoni F, Schmid G and Talkner P 2009 Diffusion in confined geometries *ChemPhysChem* **10** 45–54
[2] Reguera D, Schmid G, Burada P S, Rubi J M, Reimann P and Hänggi P 2006 Entropic transport: kinetics, scaling and control mechanisms *Phys. Rev. Lett.* **96** 130603
[3] Burada P S, Schmid G, Talkner P, Hänggi P, Reguera D and Rubi J M 2008 Entropic particle transport in periodic channels *Biosystems* **93** 16–22
[4] Burada P S, Schmid G, Reguera D, Rubi J M and Hänggi P 2007 Biased diffusion in confined media: test of the Fick–Jacobs approximation and validity criteria *Phys. Rev.* E **75** 051111
[5] Siwy Z and Fulinski A 2002 Fabrication of a synthetic nanopore ion pump *Phys. Rev. Lett.* **89** 198103
[6] Siwy Z, Kosinska I D, Fulinski A and Martin C R 2005 Asymmetric diffusion through synthetic nanopores *Phys. Rev. Lett.* **94** 048102
[7] Kosinska I D, Goychuk I, Kostur M, Schmid G and Hänggi P 2008 Rectification in synthetic conical nanopores: a one-dimensional Poisson–Nernst–Planck modeling *Phys. Rev.* E **77** 031131
[8] van Dorp S, Keyser U F, Dekker N H, Dekker C and Lemay S G 2009 Origin of the electrophoretic force on DNA in solid-state nanopores *Nat. Phys.* **5** 347–51
[9] Kullman L, Winterhalter M and Bezrukov S M 2002 Transport of maltodextrins through maltoporin: a single-channel study *Biophys. J.* **82** 803–12

[10] Berezhkovskii A M and Bezrukov S M 2005 Optimizing transport of metabolites through large channels: molecular sieves with and without binding *Biophys. J.* **88** L17–9
[11] Berezhkovskii A M, Pustovoit M A and Bezrukov S M 2007 Diffusion in a tube of varying cross section: numerical study of reduction to effective one-dimensional description *J. Chem. Phys.* **126** 134706
[12] Berezhkovskii A M, Pustovoit M A and Bezrukov S M 2009 Entropic effects in channel-facilitated transport: interparticle interactions break the flux symmetry *Phys. Rev.* E **80** 020904(R)
[13] Gammaitoni L, Hänggi P, Jung P and Marchesoni F 1998 Stochastic resonance *Rev. Mod. Phys.* **70** 223–88
[14] Burada P S, Schmid G, Reguera D, Vainstein M H, Rubi J M and Hänggi P 2008 Entropic stochastic resonance *Phys. Rev. Lett.* **101** 130602
[15] Burada P S, Schmid G, Reguera D, Rubi J M and Hänggi P 2009 Entropic stochastic resonance: the constructive role of the unevenness *Eur. Phys. J.* B **69** 11–18
[16] Burada P S, Schmid G, Reguera D, Rubi J M and Hänggi P 2009 Double entropic stochastic resonance *Eur. Phys. Lett.* **87** 50003
[17] Ghosh P K, Marchesoni F, Savel'ev S E and Nori F 2010 Geometric stochastic resonance *Phys. Rev. Lett.* **104** 020601
[18] Purcell E M 1977 Life at low reynolds number *Am. J. Phys.* **45** 3–11
[19] Hänggi P and Thomas H 1982 Stochastic processes: time-evolution, symmetries and linear response *Phys. Rep.* **88** 207–319
[20] Jacobs M 1967 *Diffusion Processes* (New York: Springer)
[21] Zwanzig R 1992 Diffusion past an entropic barrier *J. Phys. Chem.* **96** 3926–30
[22] Reguera D and Rubí J M 2001 Kinetic equations for diffusion in the presence of entropic barriers *Phys. Rev.* E **64** 061106
[23] Kalinay P and Percus J K 2006 Corrections to the Fick–Jacobs equation *Phys. Rev.* E **74** 041203
[24] Kalinay P 2009 Mapping of forced diffusion in quasi-one-dimensional systems *Phys. Rev.* E **80** 031106
[25] Bradely R M 2009 Diffusion in a two-dimensional channel with curved midline and varying width: reduction to an effective one-dimensional description *Phys. Rev.* E **80** 061142
[26] Reimann P, Van den Broeck C, Linke H, Hänggi P, Rubi J M and Pérez-Madrid A 2001 Giant acceleration of free diffusion by use of tilted periodic potentials *Phys. Rev. Lett.* **87** 010602
[27] Lindner B, Kostur M and Schimansky-Geier L 2001 Optimal diffusive transport in a tilted periodic potential *Fluct. Noise Lett.* **1** R25
[28] Reimann P, Van den Broeck C, Linke H, Hänggi P, Rubi J M and Pérez-Madrid A 2002 Diffusion in tilted periodic potentials: enhancement, universality, and scaling *Phys. Rev.* E **65** 031104
[29] Burada P S, Schmid G and Hänggi P 2009 Entropic transport: a test bed for the Fick–Jacobs approximation *Phil. Trans. R. Soc.* A **367** 3157–71
[30] Hänggi P, Talkner P and Borkovec M 1990 Reaction rate theory: fifty years after Kramers *Rev. Mod. Phys.* **62** 251–342
[31] Burada P S, Schmid G, Li Y and Hänggi P 2010 Controlling diffusive transport in confined geometries *Acta Phys. Pol.* B **41** 935–47
[32] Koenig S H 1975 *Biopolymers* **14** 2421–3